

Optimization of the signal-to-noise ratio for photoreflectance spectroscopy

U. Behn

Fachhochschule Schmalkalden, Blechhammer, 98574 Schmalkalden, Germany

A. Thamm,^{a)} O. Brandt, and H. T. Grahn^{b)}

Paul-Drude-Institut für Festkörperelektronik, Hausvogteiplatz 5-7, 10117 Berlin, Germany

(Received 24 July 2001; accepted for publication 24 August 2001)

The amplitude and the signal-to-noise ratio of photoreflectance (PR) spectra are experimentally and theoretically investigated as a function of the pump and probe intensity. The model calculations of the PR amplitude and the signal-to-noise ratio based on a simple transport model taking the shot noise of the photodetector as the only noise source confirm the experimentally observed dependencies. Increasing the probe light intensity leads to a decrease of the absolute PR background noise. At the same time, the PR amplitude decreases. This may, in particular for comparable probe and pump intensities, result in a decrease of the signal-to-noise ratio. © 2001 American Institute of Physics. [DOI: 10.1063/1.1412828]

I. INTRODUCTION

Photoreflectance (PR) spectroscopy belongs to one of the standard techniques to characterize bulk semiconductors and thin film semiconductor heterostructures.¹⁻³ In the last few years, PR spectroscopy has also been applied to group-III nitrides such as GaN, (In, Ga)N, (Al, Ga)N, and related heterostructures due to their possible application in blue and UV light-emitting devices and high-power electronics. PR investigations have been used to determine the energy gap, the temperature dependence of the energy gap, the bowing parameter, the piezoelectric fields, etc., in these materials. The accuracy of the parameters estimated from fitting the room- and low-temperature PR spectra depends sensitively not only on the validity of the line shape model used and the modulation mechanism, but also on the signal-to-noise ratio (S/N).

In order to optimize the signal-to-noise ratio, it is necessary to quantitatively determine the dependencies of the PR signal $\Delta R/R$ and the PR noise level on the probe and the pump light intensity. By carefully designing the PR setup and minimizing the external noise sources such as acoustic noise (e.g., due to cooling fan vibrations or stepper motor noise in the monochromator), power line noise, etc., the noise level of the PR spectra can be reduced close to the physical limit. This limit is given by the intrinsic noise sources, most importantly the shot noise of the detector.

In this paper, we determine experimentally and theoretically the PR amplitude and the signal-to-noise ratio of the PR spectra as a function of pump and probe light intensity. We use a simple transport model to calculate the photovoltage caused by the pump and probe light and take shot noise as the only noise source. It is well known that increasing the probe light intensity normally results in an increase of the signal-to-noise ratio for the PR spectra. We will demonstrate

that under certain modulation conditions, in particular for comparable probe and pump intensities, an increase of the probe light intensity can even lead to a decrease of the signal-to-noise ratio. The experimental PR data recorded at room temperature are confirmed by the calculated dependencies of $\Delta R/R$ and S/N on probe and pump light intensities. Although the experiments and calculations are performed for a particular material (GaN), similar results are also expected for other materials such as GaAs, (Al, Ga)As, InP, (In, Ga)As, etc.

After describing the experimental setup and the investigated sample in Sec. II, we determine quantitatively the PR background noise level in Sec. III. The calculated PR amplitude and resulting signal-to-noise ratio are presented in Sec. IV, followed by a comparison with the experimental results and a discussion in Sec. V. Finally, we summarize the results in Sec. VI.

II. EXPERIMENT

We performed photoreflectance measurements using a PR setup containing three monochromators as shown in Fig. 1. The light of a 75 W Xe lamp is dispersed by monochromator 1 (Zeiss Jena, $f=2075$ mm) and directed onto the sample under nearly normal incidence. The reflected light is passed through monochromator 2 (Acton Research, $f=275$ mm), which acts as an adjustable, narrow bandpass filter. It is used to remove spurious light such as photoluminescence or scattered light. The detector is an UV-enhanced Si photodiode. The signal is preamplified and detected by conventional lock-in technique. The monochromatic pump light is generated by dispersing the light of a 150 W Xe lamp using monochromator 3 (Zeiss Jena, $f=400$ mm). Excitation densities up to 6 mW cm^{-2} can be utilized with this setup. The excitation wavelength λ for recording the PR spectra is set to 340 nm (3.646 eV).

The investigated sample consists of a 1.7- μm -thick GaN layer deposited directly onto 6H-SiC(0001) by reactive molecular-beam epitaxy, utilizing an unheated injector for

^{a)}Present address: Infineon Technologies Dresden GmbH & Co. OHG, Koenigsbruecker Strasse 180, 01099 Dresden, Germany.

^{b)}Electronic mail: htg@pdi-berlin.de

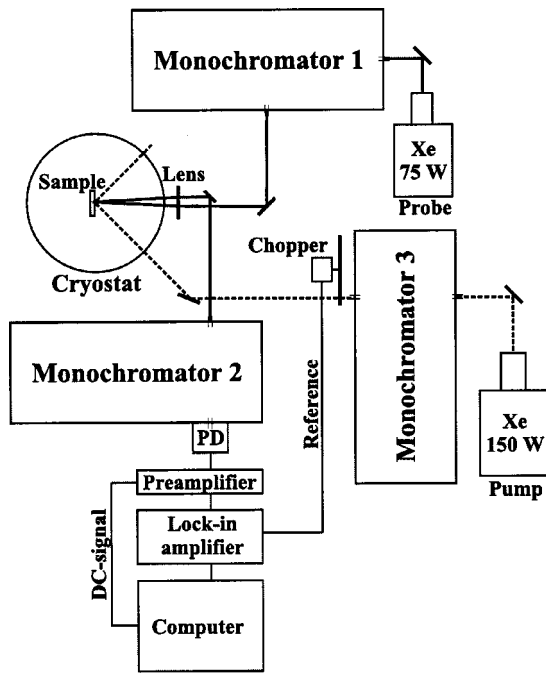


FIG. 1. Schematic diagram of the photoreflectance setup. PD denotes the photodiode.

introducing NH_3 into the system. Details of the growth conditions can be found in Ref. 4. The background electron concentration, as determined by capacitance voltage profiling, amounts to $2 \times 10^{17} \text{ cm}^{-3}$.

III. DETERMINATION OF THE NOISE LEVEL

Inevitable intrinsic noise sources in PR spectroscopy are the photodetector shot noise, the Johnson noise of the feedback resistor of the current preamplifier, and the $1/f$ noise. By carefully choosing the modulation frequency and the transresistance of the preamplifier, the $1/f$ noise and the Johnson noise can be kept much smaller than the shot noise I_S , which can be expressed as⁵

$$I_S = \sqrt{2eI_{\text{PD}}\Delta f}, \quad (1)$$

where e denotes the elementary charge, I_{PD} the current of the photodetector, and Δf the noise bandwidth, which can be determined from the lock-in amplifier time constant τ (6 dB/octave filter) using

$$\Delta f = \frac{1}{2\pi\tau}. \quad (2)$$

Taking the shot noise as the only noise source for the PR spectra, the PR background noise can then be determined from

$$\left(\frac{\Delta R}{R}\right)_{\text{noise}} = \frac{I_S}{I_{\text{PD}}} = \frac{\sqrt{2eI_{\text{PD}}\Delta f}}{I_{\text{PD}}} = \sqrt{\frac{2e\Delta f}{I_{\text{PD}}}} \propto \sqrt{\frac{1}{I_{\text{PD}}}}. \quad (3)$$

Since I_{PD} is proportional to the probe light intensity, this equation implies that increasing the probe light intensity and therefore I_{PD} by a factor of 4 decreases the PR background noise by a factor of 2. If we take, for example, a typical photodetector current of $I_{\text{PD}} = 8 \text{ nA}$ and a typical noise band-

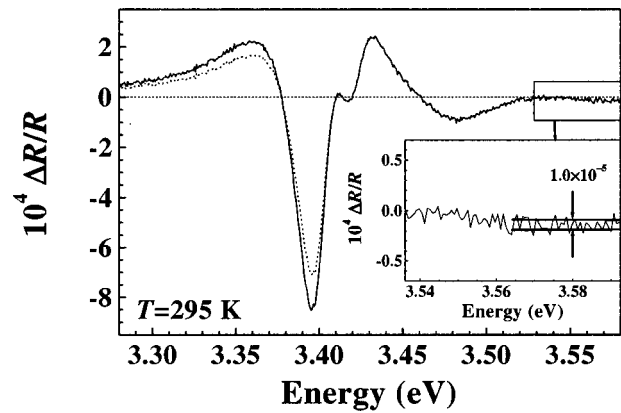


FIG. 2. Room-temperature PR spectrum of the GaN film measured with a probe light intensity $P_{\text{probe}} = 0.15 \text{ mW cm}^{-2}$, a pump light intensity $P_{\text{pump}} = 5 \text{ mW cm}^{-2}$, a lock-in time constant $\tau = 0.3 \text{ s}$, and an averaging time $t = 1 \text{ s}$ per data point. The dotted line shows the same spectrum corrected for a constant modulation voltage.

width $\Delta f = 1 \text{ Hz}$, we obtain a shot noise current of $I_S = 50.6 \text{ fA}$ resulting in a PR background noise level of $(\Delta R/R)_{\text{noise}} = 6.33 \times 10^{-6}$.

Figure 2 shows a PR spectrum of a GaN film recorded at room temperature. The line shape of this spectrum is Franz-Keldysh like, exhibiting the typical Franz-Keldysh oscillations for energies $E > 3.45 \text{ eV}$, but it is also influenced by electron-hole interactions as expected from the room temperature absorption data of GaN,⁶ which show a clear excitonic resonance. The current of the photodiode used for this spectrum is about 8 nA as in the above-mentioned numerical example. Using the noise option of the lock-in amplifier with a bandwidth of $\Delta f = 1 \text{ Hz}$, we measure a noise current of $(57 \pm 7) \text{ fA}$, which is in very good agreement with the shot noise level calculated from the photodetector current. However, for this spectrum, we actually used a lock-in amplifier time constant of $\tau = 0.3 \text{ s}$ resulting in a noise bandwidth of $\Delta f = 0.53 \text{ Hz}$. Therefore, the PR background noise level calculated from Eq. (3) becomes $(\Delta R/R)_{\text{noise}} = 4.5 \times 10^{-6}$, which is about half of the noise level subjectively estimated from the experimental spectra as shown in the inset of Fig. 2. While the subjective estimation of the noise directly from the spectrum corresponds to the amplitude of the noise level, the noise is actually related to the variance of the PR fluctuations.

Although Eq. (3) shows that an increase of the probe light intensity results in a decrease of the background noise level, the quality of a PR spectrum is rather determined by the signal-to-noise ratio S/N than by the absolute noise level. We define in the following S/N as the ratio between the PR amplitude and the PR background noise level, i.e.,

$$S/N = \frac{(\Delta R/R)_{\text{amp}}}{(\Delta R/R)_{\text{noise}}}. \quad (4)$$

IV. DETERMINATION OF THE PR AMPLITUDE AND THE SIGNAL-TO-NOISE RATIO

We calculate the PR amplitude and the PR signal-to-noise ratio for GaN films assuming shot-noise-limited PR

spectra and using a simple transport model for determining the surface photovoltage. The following four assumptions are made. First, the modulation mechanism of the PR is based on photoinduced generation of electron–hole pairs and screening of the surface electric field and is therefore electric field modulation. Second, the electric field and the band bending in the depletion layer near the surface are described by the Schottky model. Third, the modulation is assumed to be steady state, i.e., the typical relaxation and drift times are short compared to the modulation period. Fourth, in the low modulation limit, the PR amplitude is proportional to the surface modulation voltage V_m .^{7,8}

The photovoltage can be expressed using transport theory^{3,9,10} by

$$V_S = \frac{\eta k_B T}{e} \ln \left[\frac{J_{PC}}{J_{ST}(T)} + 1 \right], \quad (5)$$

where η is an ideality factor, k_B Boltzmann’s constant, and $J_{ST}(T)$ the saturation (dark) current density. J_{PC} denotes the photoinduced current density, which can be expressed as⁹

$$J_{PC} = \frac{e P \gamma (1 - R)}{\hbar \omega} \left(1 - \frac{\exp(-\alpha W)}{1 + \alpha L_D} \right), \quad (6)$$

where P denotes the pump or probe intensity, γ the quantum efficiency, R the reflectivity at the surface, $\hbar \omega$ the photon energy, α the absorption coefficient, W the width of the depletion layer, and L_D the diffusion length of the minority carriers. The saturation current density is given by^{3,9}

$$J_{ST} = \frac{A^{**} T^2}{1 + B T^{3/2}} \exp \left[- \frac{e V_F(T)}{k_B T} \right], \quad (7)$$

where A^{**} denotes the modified Richardson constant and B a constant related to the saturation velocity. V_F is the surface Fermi voltage. In the calculations based on Eqs. (5)–(7), we used the experimental absorption data of Fischer *et al.*⁶ and the following parameters: $T = 295$ K, $\eta = 1$, $A^{**} = 2.4 \times 10^5$ A(m K)⁻², $B = 4.62 \times 10^{-5}$ K^{-3/2}, $L_D = 2.8 \times 10^{-7}$ m,¹¹ and $V_F(295 \text{ K}) = 0.7$ V.

In photoreflectance measurements, both the pump and the probe light contribute to J_{PC} . Depending on the chopper state (pump on or off), the sample is modulated between the light levels P_{probe} (pump off) and $P_{\text{probe}} + P_{\text{pump}}$ (pump on), resulting in the two photovoltages V_S^{off} and V_S^{on} . Using Eq. (5), the modulation voltage V_m is then given by

$$V_m = V_S^{\text{on}} - V_S^{\text{off}} = \frac{\eta k_B T}{e} \left(\ln \left[\frac{J_{\text{probe}} + J_{\text{pump}}}{J_{ST}} + 1 \right] - \ln \left[\frac{J_{\text{probe}}}{J_{ST}} + 1 \right] \right). \quad (8)$$

This expression can be transformed into

$$V_m = \frac{\eta k_B T}{e} \ln \left[1 + \frac{J_{\text{pump}}}{J_{\text{probe}} + J_{ST}} \right]. \quad (9)$$

Assuming that the amplitude of the PR signal $(\Delta R/R)_{\text{amp}}$ is proportional to V_m , it can be described by

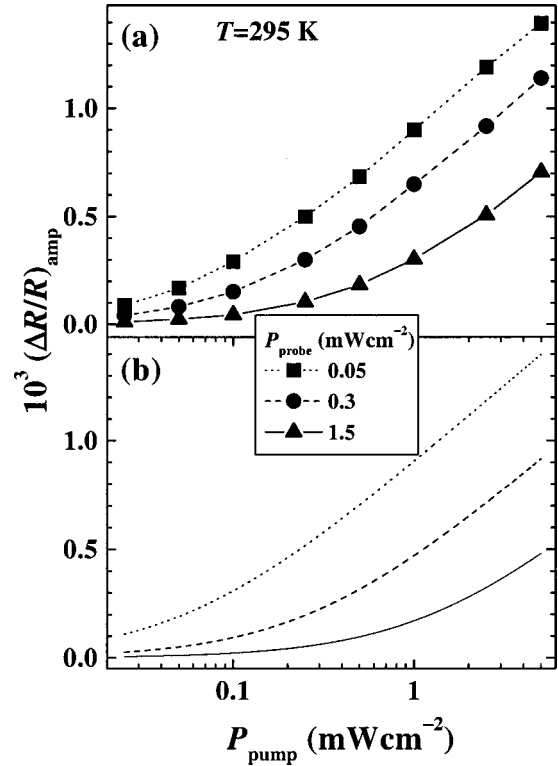


FIG. 3. (a) Experimental and (b) calculated curves using Eqs. (5)–(10) of the PR amplitude $(\Delta R/R)_{\text{amp}}$ as a function of the pump intensity P_{pump} for three different values of the probe intensity P_{probe} as indicated.

$$\left(\frac{\Delta R}{R} \right)_{\text{amp}} = C_1 V_m, \quad (10)$$

where C_1 is a constant depending on the actual line shape (e.g., Franz-Keldysh like, first derivative excitonic or third derivative) and the line broadening determined by temperature and crystal quality.

Using Eqs. (3) and (4), the signal-to-noise ratio can then be expressed by

$$S/N = C_1 V_m \sqrt{\frac{I_{PD}}{2e \Delta f}}. \quad (11)$$

Since the photodetector current is directly proportional to the probe intensity, the signal-to-noise ratio can be written as

$$S/N = C_2 V_m \sqrt{P_{\text{probe}}}, \quad (12)$$

where C_2 denotes a second constant and P_{probe} the intensity of the probe light.

V. COMPARISON BETWEEN EXPERIMENTAL AND CALCULATED PR AMPLITUDES AND SIGNAL-TO-NOISE RATIOS

Figure 3(a) shows the measured dependence of the PR amplitude $(\Delta R/R)_{\text{amp}}$ on the pump intensity (logarithmic scale) for three different levels of the probe intensity. For large pump intensities ($P_{\text{pump}} \gg P_{\text{probe}}$), the PR signal scales logarithmically with the pump intensity. This observation is very well reproduced by the numerical evaluation of Eqs. (5)–(10) displayed in Fig. 3(b). Furthermore, the variation of the dependence of $(\Delta R/R)_{\text{amp}}$ on P_{pump} for different probe

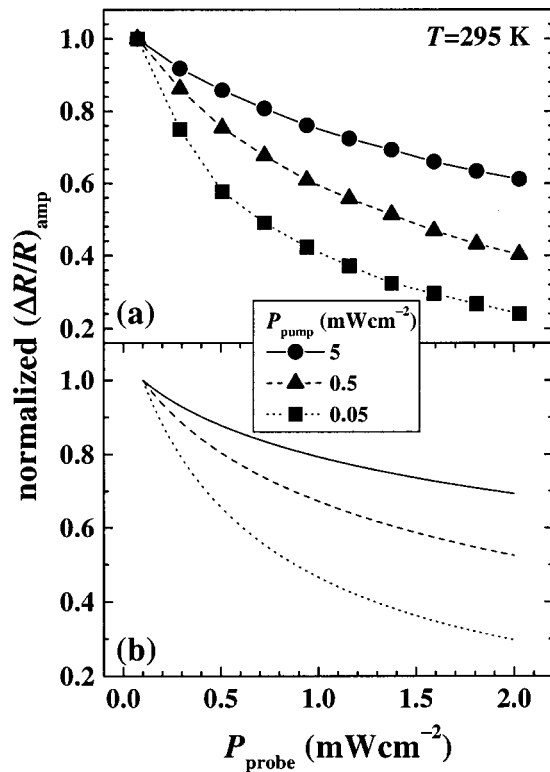


FIG. 4. (a) Experimental and (b) calculated curves using Eqs. (5)–(10) of the normalized PR amplitude $(\Delta R/R)_{\text{amp}}$ as a function of probe intensity P_{probe} for three different values of the pump intensity P_{pump} as indicated. The curves were normalized by taking the $(\Delta R/R)_{\text{amp}}$ value for the smallest value of P_{pump} to be one.

intensities is also in excellent agreement with the experimental observation. Finally, our results confirm the reports of Wagner *et al.*¹² and Hughes *et al.*¹³

In Fig. 4(a), the experimentally observed $(\Delta R/R)_{\text{amp}}$ is plotted as a function of P_{probe} on a linear scale for three different pump intensities. $(\Delta R/R)_{\text{amp}}$ has been normalized to the value for the smallest probe intensity. Again, the calculated result based on Eqs. (5)–(10), which is shown in Fig. 4(b), agrees very well with the experimental observation. Figure 4 and Eq. (9) show that an increase of the probe intensity or J_{probe} , while keeping the pump intensity or J_{pump} as well as J_{ST} constant, leads to a decrease of the PR amplitude. Therefore, a PR setup utilizing white light as the probe (as used, e.g., in Refs. 14 and 15) results in a reduced PR signal and, consequently, in a poorer signal-to-noise ratio. The much larger intensity of the undispersed white probe light in comparison to spectrally filtering the probe light to a very narrow spectral range strongly increases P_{probe} . Therefore, the modulation voltage and the PR amplitude are strongly reduced as shown in Fig. 4.

Another consequence of the dependence of the PR amplitude on the probe intensity shown in Fig. 4 is the spectral variation of the modulation voltage, even if the pump light intensity remains constant. Near the energy gap, the absorption coefficient α exhibits a strong increase with increasing photon energy E_{photon} . Therefore, with increasing E_{photon} , more and more probe light is absorbed leading to a decrease of the modulation voltage (cf. Fig. 4), which will result in a

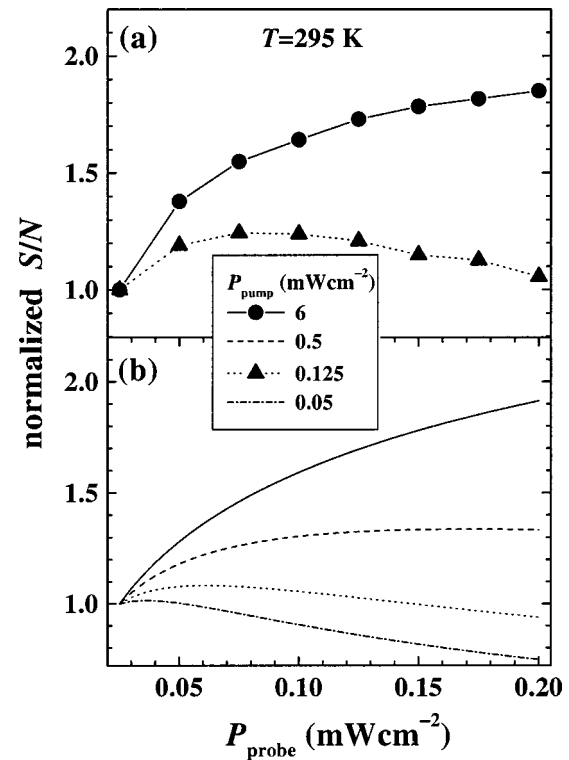


FIG. 5. (a) Experimental and (b) calculated curves using Eqs. (4)–(12) of the normalized signal-to-noise ratio as a function of probe intensity P_{probe} for different values of the pump intensity P_{pump} as indicated. The experimental curves were obtained by dividing the PR amplitude by the noise measured with a noise bandwidth of $\Delta f=1\text{ Hz}$. The curves were normalized by taking the S/N value for the smallest value of P_{probe} to be one.

change of the PR line shape compared to a spectrum obtained with a constant modulation voltage amplitude as in electroreflectance spectroscopy. In Fig. 2, the dotted line shows the measured PR spectrum corrected for constant modulation voltage by taking into account the spectral dependence of the absorption coefficient α .⁶ This corrected spectrum shows a reduced PR signal, in particular near and below the energy gap. Our calculations show that this effect becomes even more pronounced at low temperatures, where it could lead to considerable errors in the estimation of excitonic transition energies and broadening parameters by fitting the uncorrected low-temperature PR spectra.

Finally, we will compare the experimental and calculated results for the signal-to-noise ratio. As mentioned previously, increasing the probe intensity reduces the absolute PR noise level as shown in Eq. (3). At the same time, it decreases the PR amplitude. Therefore, the signal-to-noise ratio may even decrease with increasing probe intensity. Figure 5(a) shows the measured S/N as a function of P_{probe} for two different values of P_{pump} . S/N has been normalized to the value for the smallest probe intensity. We can distinguish two regions. For large pump intensities ($P_{\text{pump}} \gg P_{\text{probe}}$), the signal-to-noise-ratio increases with increasing P_{probe} following the square-root dependence on P_{probe} as predicted by Eq. (12). However, for values of P_{pump} in the same range as P_{probe} , we clearly observe a very different behavior. When P_{probe} becomes larger than P_{pump} , the signal-to-noise ratio decreases with increasing P_{probe} . Again, the calculations based on Eqs.

(4)–(12) shown in Fig. 5(b) clearly support the observed dependence. For very small values of P_{pump} , the signal-to-noise ratio for large values of P_{probe} becomes even smaller than the initial value.

VI. CONCLUSIONS

We have measured the amplitude and the signal-to-noise ratio as a function of the pump and probe intensity for photoreflectance spectroscopy. The model calculations of the PR amplitude and the signal-to-noise ratio based on a simple transport model taking the shot noise of the photodetector as the only noise source confirm the experimentally observed dependencies on pump and probe intensity. Increasing the probe light intensity leads to a decrease of the absolute PR background noise. At the same time, the PR amplitude decreases. This may, in particular for comparable probe and pump intensities, result in a decrease of the signal-to-noise ratio.

We suggest that the observed decrease of the PR amplitude with increasing probe intensity could be the main reason for the poor signal-to-noise ratio obtained for PR setups using undispersed white light as the probe light. The spectral variation of the absorbed probe light intensity with increasing photon energy near the absorption edge leads to a spectrally varying modulation voltage in the PR spectra. This can result in a change of the line shape in comparison to spectra obtained with a constant modulation voltage so that this effect should be taken into account for line shape investigations, in particular for fitting low-temperature excitonic spectra.

The excellent quantitative agreement between the experimental and calculated data without any fitting parameters

suggests that the applied theoretical model for the surface photovoltage, which was already successfully used for the estimation of the surface Fermi level pinning of GaAs,^{3,9} is also applicable to GaN films.¹⁰ We believe that the obtained results can also be useful for other materials such as GaAs, (Al,Ga)As, InP, (In,Ga)As, etc.

¹See, e.g., O. J. Glembocki and B. V. Shanabrook, in *Semiconductors and Semimetals*, edited by D. G. Seiler and C. L. Littler (Academic, New York, 1992), Vol. 36, p. 221.

²See, e.g., F. H. Pollak, in *Handbook on Semiconductors*, edited by M. Balkanski (North Holland, New York, 1994), Vol. 2, p. 527.

³H. Shen and M. Dutta, *J. Appl. Phys.* **78**, 2151 (1995).

⁴A. Thamm, O. Brandt, Y. Takemura, A. Trampert, and K. H. Ploog, *Appl. Phys. Lett.* **75**, 944 (1999).

⁵See, e.g., S. M. Sze, *Physics of Semiconductor Devices*, 2nd ed. (Wiley, New York, 1981).

⁶A. J. Fischer, W. Shan, J. J. Song, Y. C. Chang, R. Horning, and B. Goldenberg, *Appl. Phys. Lett.* **71**, 1981 (1997).

⁷T. Kanata, M. Matsunaga, H. Takakura, and Y. Hamakawa, *J. Appl. Phys.* **68**, 5309 (1990).

⁸R. A. Batchelor, A. C. Brown, and A. Hammet, *Phys. Rev. B* **41**, 1401 (1990).

⁹X. Yin, H.-M. Chen, F. H. Pollak, Y. Chan, P. A. Montano, P. D. Kirchner, G. D. Pettit, and J. M. Woodall, *J. Vac. Sci. Technol. A* **10**, 131 (1992).

¹⁰U. Behn, A. Thamm, O. Brandt, and H. T. Grahn, *J. Appl. Phys.* **87**, 4315 (2000).

¹¹Z. Z. Bandić, P. M. Bridger, E. C. Piquette, and T. C. McGill, *Appl. Phys. Lett.* **72**, 3166 (1998).

¹²R. E. Wagner and A. Mandelis, *Phys. Rev. B* **50**, 14228 (1994).

¹³P. J. Hughes, B. L. Weiss, and T. J. C. Hosea, *J. Appl. Phys.* **77**, 6472 (1995).

¹⁴S. Chichibu, H. Okumura, S. Nakamura, G. Feuillet, T. Azuhata, T. Sota, and S. Yoshida, *Jpn. J. Appl. Phys., Part 1* **36**, 1976 (1997).

¹⁵C. Wetzels, T. Takeuchi, S. Yamaguchi, H. Katoh, H. Amano, and I. Akasaki, *Appl. Phys. Lett.* **73**, 1994 (1998).